Weighted Least Squares for Visualization of Scanned Point Clouds

Marc S. Goldstein[1] and Robert V. Fleisig[2]

[1]McMaster University, goldstms@mcmaster.ca
[2]McMaster University, robert@mcmaster.ca

ABSTRACT

This paper describes several improvements to implicit surface fitting over point clouds. Noisy stamped part point cloud data gathered by both a laser digitizer scanning system and a stereo vision sensor is processed using a method based on the weighted least squares algorithm. Two kernel functions are proposed: one using an enhanced sphere-of-influence graph (SIG) method to determine nearest neighbours; and a second using an improved Gaussian kernel. Automatic bandwidth adjustment is implemented for both methods. A method of incorporating a scalar attribute at each data point, which can represent any desired quantity and relate it to the surface at that point, is introduced. In this case surface strain data was gathered and processed by the scanning system, with a resulting thickness strain measurement calculated at each point. This strain data was used to introduce a temperature plot style colour map over the surface, allowing for fast and simple analysis of the strain of the formed part.

Keywords: Weighted least squares; surface reconstruction; unorganized point cloud; strain analysis; visualization

1. INTRODUCTION

To ensure part quality in sheet metal forming processes, inspection to verify adherence to both strain and geometry criteria is required. Laser digitizer and stereo vision systems [7],[21] have been developed to quickly analyze formed sheet metal parts such as those shown in Fig. 1, and produce correlated geometry and strain data in the form of unorganized point clouds. The past decade has seen significant development in the area of 3D scanning devices and therefore a corresponding development in the treatment of the point cloud data they produce. For the point cloud to be of use in analyzing the visualization of the part, a surface must be developed to clearly represent the boundary of the part. The desire is for this defined surface to be as close as possible to the actual surface, while eliminating the effects of noise introduced through registration of the data and with the shortest possible processing time for the algorithm.

(a) Laser digitizer part with circular grid (b) Stereo vision camera part with square grid

Fig. 1. Laser digitizer and stereo vision sensor test stamped sheet metal parts. The insets in each figure show the grid patterns.

The basis for this paper is the weighted least squares (WLS) implicit surface fitting function. Weighted orthogonal least squares (WOLS) is an improvement on the standard WLS algorithm that uses the square sum of the orthogonal distance from each point P_i to the line C_i. A significant improvement on the WLS method was made by Klein [11], who used a proximity graph distance kernel rather than the standard Euclidean kernel, allowing for automatic bandwidth adjustment to account for variations in local data density.

In this paper, several improvements are made to both the WLS and the sphere-of-influence graph (SIG) methods. Changes are required because the real part data used in this paper, gathered by 3D scanning systems, is non-uniform and of varying density. In the case of the laser digitizer data, sweeps of the laser beam often cross each other at small angles. With the stereo camera system the same physical point on an object can be seen in many images and due to noise can appear to be a set of different, but very closely grouped, points. These factors both lead to wide variations in the density of points across a data set. New distance kernels are developed and tested, including a method of automating the size of r, the parameter which represents the r^{th} nearest neighbour in the SIG method. In addition to the implicit surface development, a scalar attribute is related to each data point. In this case, the scalar is the measured thickness strain of the part, gathered by the scanning systems, which is used to create a 3D temperature plot display of strain over the part surface.

The remainder of this paper is organized as follows. Section 2 deals with related work and provides background information. Section 3 deals in more detail with the WLS method and incorporates the SIG. The improved Gaussian surface model is explained in Section 4. Section 5 deals with the introduction of a scalar attribute – in this case strain data – to the surface model. Section 6 discusses the results to date and conclusions are presented in Section 7.

2. RELATED WORK

A point cloud is a set of points that have been collected, usually by 3D scanning apparatus, from an actual part surface. Surface reconstruction is the attempt to organize point cloud data for visualization. Due to the increased use of scanners in recent years, much research has been done in the area of surface reconstruction. We initially investigated radial basis functions [5-6], but they were deemed too computationally complex for the large point cloud data sets used in this paper. Surfels, surface element extensions of a local area of points to form a piece-wise surface [18-19], are another form of surface plotting, but one that is again not suited to the data used. Other approaches for reconstructing surfaces from unorganized point data are also available [3],[9].

The least squares method of dimensional model fitting can be traced back to Gauss in 1809 [8] and is the foundation for this paper. The LSM minimizes the square of the distance between a particular data point and the desired surface; the surface is defined as the zero set of an implicit function that is constructed from the point cloud data. The weighted least squares method is an improvement of the standard LSM and was developed by McLain [15-16] and then carried forward by Levin [13] who discusses the mathematics of WLS in detail. For a local neighbourhood of points P_i, WLS computes a regression line C_i at each data point P_i which best fits the points in that neighbourhood using a weighted regression method. The point P_i is then moved to the point P_i' and the process continues. Further research in the area of WLS was carried out by Lee [12] and again by Levin [14]. The WLS method is best suited to a thin cloud of points, where the points vary little from the best fit curve or surface, for which the results are very good. However, point sets of varying thickness and density and with unwanted noise are not well handled by the WLS method. Lee has made several improvements, mainly to the distance kernel. The standard kernel used is the Euclidean distance between points, but improved methods better relate the distance along the surface between data points. Also, different weighting functions are used with the main criterion being that the weighting function must generate larger penalties for points further from the data point in question, P_*. Lee's weighting function is a finite kernel; it includes a condition to exclude points farther than some specified radial distance h from P_*. Ahn improved upon the WLS model by defining that the lines from data points to the reconstructed surface be orthogonal to the surface, thus creating the weighted orthogonal least squares (WOLS) model for implicit surface fitting [1-2]. Ahn developed two WOLS algorithms, the distance-based algorithm and the coordinate-based algorithm. These WOLS algorithms are more versatile and efficient than the previous WLS surface fitting methods.

With the basic WLS and WOLS implicit surface fitting methods developed, recent research has been related to improved distance kernels to better relate the unorganized data points. One common approach is to use proximity graphs rather than the Euclidean distance. Many proximity graphs have been studied, including the Delaunay and nearest neighbour graphs, the α-shape and the sphere-of-influence graph, or SIG [10]. The SIG has shown the most promise and has been studied from various points of view, often in the field of optical character recognition [4],[17] and also in the development of surfaces from point clouds [11]. With the SIG method, each data point is the centre of an open sphere of radius equal to the distance between that point and its nearest neighbour, and two points are adjacent if their spheres intersect. This can be expanded to the r-SIG, in which the r^{th} nearest neighbour is used, thereby increasing the number of connections between data points. Klein uses the weighted least squares method as a basis for surface fitting and experiments with a variety of distance kernels, concluding that the SIG proximity graph,

and more specifically the *r*-SIG, produces the surface closest to that of the original part. Klein also introduced automatic bandwidth computation and automatic boundary detection to determine the outer edge of the surface as extensions to the SIG calculation.

3. LEAST SQUARES WITH SIG SURFACE MODEL

In the majority of the current work the data sets used are relatively simple. Implicit surface fitting to a large unorganized point cloud set gathered from a part with many complex surface changes is more difficult. Initially we used the standard WLS method with a point cloud gathered from a dome-shaped stamped metal part.

3.1 Point Cloud Data Sets

We used two types of data sets for this paper, both gathered by 3D scanning systems from real parts. In all cases, the parts were stamped sheet metal and a circular or square grid pattern was printed on the sheet prior to stamping. The spacing of both the circle and the square grids was initially 2.54 mm. The patterns would be deformed after stamping, with the squares and circles deforming based on the local strain in the material, as shown in Fig. 1. The circles become ellipses after stamping. The resultant point cloud data sets are shown in Fig. 2.

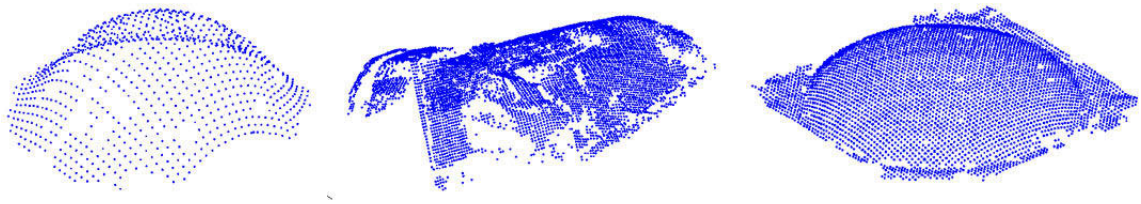

a) Laser digitizer data from test dome 1 (b) Laser digitizer data from stamped part (c) Stereo vision data from test dome 2
Fig. 2. Unorganized point cloud data gathered from actual parts by 3D scanning systems.

We used a scanning laser digitizer to gather some of the data used. This laser system uses internal rotating mirrors to guide the laser beam through a planar arc, gathering both 3D position and intensity data for many points through each arc. The digitizer head is moved by a coordinate measuring machine in unison with the laser plane travel, so that the resulting raw data is formed by many parallel lines of points. The intensity data is used to record the locations of the deformed ellipses, and post-processing of the data results in an unorganized cloud of four-dimensional data with each point including the three Cartesian coordinates and the corresponding thickness strain of one ellipse. The combination of the laser arc movement and the CMM movement leads to regular grids of data points, and in order to fully scan the part these grids must overlap. The resulting data therefore has irregular variations in point density. Where only one grid of data has been collected for an area of the part the grid is evenly distributed, but when two or more of these grids of data intersect, there are often several points in very close proximity. Many surface fitting approaches have problems with this type of variation in density and do not smoothly interpret the entire part surface.

Fig. 3. Repeated data points due to multiple stereo vision images used to capture data set.

We also used data from a 3D stereo vision sensor, which uses two digital cameras to simultaneously capture an image of a part. The two cameras give depth to the data and allow for the same four-dimensional data to be gathered. The stereo vision sensor must take many images of a part, and these images are combined by the process of registration to gather a complete, unorganized point cloud of data to represent the surface of the part. With stereo vision data the same point is often imaged from several different points of view, and the resulting data contains many points in very close proximity which are in fact the same point. Fig. 3 shows what is in reality only two data points, but each point is

repeated several times. This varies the local density of the part in much the same way as the laser grid patterns do, but often to an even greater extent, with some points being repeated as many as 10 to 15 times. Again, surface interpolation approaches generally do not produce a smooth result over data with this type of variation in density.

Both laser digitizer and stereo vision sensor produced data therefore have large variations in the local density of the unorganized point clouds. This is a complication that greatly reduces the effectiveness of many previous surface fitting approaches, as a constant bandwidth parameter *h* does not suit this variation in density. Also, all of the data sets used have substantial holes, which result in holes in the surface. These holes are beyond what can be corrected accurately by surface fitting methods and must be addressed by improving the 3D scanning systems themselves. The fourth dimension of the data represents the thickness strain of the part. This is a scalar quantity that will be overlaid onto the surface to show strain information in terms of a colour temperature plot.

3.2 WLS Surface Model

We initially implemented the standard WLS method. An implicit function is defined to represent the surface. The point cloud **P** containing *N* points P_i in R^3 is given. The point P_* is the point on the surface for each cloud point P_i. The surface is then described as the zero set $S = \{P_* | f(P_*) = 0\}$ of the implicit function, Eqn. (1), such that a(P_*) is the weighted average of all points P_i, Eqn. (2).

$$f(P_*) = n(P_*) \cdot (a(P_*) - P_*) \cdot \tag{1}$$

$$a(P_*) = \frac{\sum_{i=1}^{N} w_i(\|P_* - P_i\|) P_i}{\sum_{i=1}^{N} w_i(\|P_* - P_i\|)} . \tag{2}$$

The weighting function w_i determines the relative weights of all points with respect to calculating the surface at the current data point P_i. This is also called the weighting kernel and there are several common kernels, such as the Gaussian kernel, Eqn. (3). The corresponding Euclidean distance calculation is given in Eqn. (4).

$$w_i = e^{-r^2/h^2} \tag{3}$$

$$r = \|P_* - P_i\| \tag{4}$$

The real constant *h*, which represents the bandwidth of the kernel, must be determined based on testing and is sensitive to the type of data used. This constant allows for the tuning of the influence of points, and is an adjustment to the weighting function. The weighting function must satisfy the criteria that those points farther from P_* have less influence on the surface at point P_*. To this end, the weighting function can also be limited such that points outside the range of *h* can be neglected if deemed to be of little influence on the surface. This can be done with a cubic weighting function, shown in Eqn. (5). The choice of either of these functions, or of other functions such as the tricube weight function, has been shown to have little effect on the resulting surface definition [11].

$$w_i = \begin{cases} 2\frac{r^3}{h^3} - 3\frac{r^2}{h^2} + 1, & r < h \\ 0, & r \geq h \end{cases} \tag{5}$$

The normal n(P_*) is defined as the direction of smallest weighted covariance, and is determined by the weighted least squares method. In other words, for a fixed P_* it minimizes Eqn. (6) under the constraint of a unit normal, $\|n(P_*)\| = 1$.

$$\sum_{i=1}^{N} (n(P_*) \cdot (a(P_*) - P_i))^2 w_i(\|P_* - P_i\|) \tag{6}$$

The normal $n(P_*)$ is the smallest eigenvector of the centred covariance matrix **B**, whose entries are b_{ij},

$$b_{ij} = \sum_{k=1}^{N} w_i\left(\left\|P_* - P_k\right\|\right)\left(P_{k_i} - a(P_*)_i\right)\left(P_{k_j} - a(P_*)_j\right) \tag{7}$$

The solution method implemented to solve the WLS problem is based on that of Ahn [1]. The method is an iterative routine to solve a non-linear equation to find a point on a surface. An initial guess at a point near the surface, P_*, is projected onto the surface and then this projected point is used as the new estimate of the point on the surface, and projected again. When the change in distance between successive projections is suitably small, the system has converged to find the point P_* on the surface, which relates to the data point P_i. Generally, the solution converges very quickly, often within three to four iterations depending on the local noise in the data.

3.3 SIG Model

The weighted least squares surface fitting method as described to this point uses a Euclidean distance kernel, Eqn. (4), that does not necessarily follow the topology of the surface but rather determines the three dimensional distance between two points. The path along the surface between the two points, called the geodesic distance, is commonly longer than the Euclidean distance but we do not have a defined surface to follow. Instead proximity graphs are used. Klein [11] found the sphere-of-influence graph (SIG), although less used than others, to be the best performing proximity graph for implicit surface fitting. The SIG method [4],[17] is used to determine if a sphere of influence centred at each data point intersects with the sphere of other data points, and if so the two points are connected by an edge. Mathematically, for each point P_i, the distance d_i to the nearest neighbour is determined by calculating the distance between that point and all other points P_j, and then an edge is connected between any two points P_i and P_j if

$$\left\|P_i - P_j\right\| \le d_i + d_j \tag{8}$$

The standard SIG model connects points only if their distance apart is less than the sum of the distances to their respective nearest neighbours. Thus, the SIG is heavily dependant on the local density of the data. If a small region has a very high density of points, there will not be many connections between this region and points outside of this region. To improve the performance in this type of situation, Klein used the *r*-SIG method [11]. Instead of calculating the distance to the nearest neighbour, this version uses the distance to the r^{th} nearest neighbour, where r is a constant determined to suit the data set. The distance d_i from the original point to the r^{th} nearest neighbour will increase with increasing r, so that as r increases more points are connected to form edges based on Eqn. (8). Klein's intention was for the *r*-SIG method to fill holes in the data and produce a more evenly connected structure than would be possible with the simple SIG method. Common choices for r are in the range of $r = 3$ to $r = 7$. Selecting a value of r which is too small eliminates the effectives of the *r*-SIG method and effectively reduces it to the SIG method, while too high an r value connects data points which are in fact quite far from each other and should not be connected. Klein also used stochastic pruning of the connections to eliminate any overly long outlier connections between data points. Fig. 4 shows the results of Klein's *r*-SIG method applied to a subset of the stereo vision data set shown in Fig. 2(c). When $r = 1$, no connections are made due to the repeated data points, as shown in Fig. 3. As r progresses through the values of 3, 5 and 7, the results steadily improve as fewer and fewer points are duplicated more than 3 or 5 times. When $r = 7$, nearly all possible connections are made, as the remaining holes were present in the raw data as well. The last case exhibits no overly long connections even though the holes are filled, showing the effectiveness of the pruning routine.

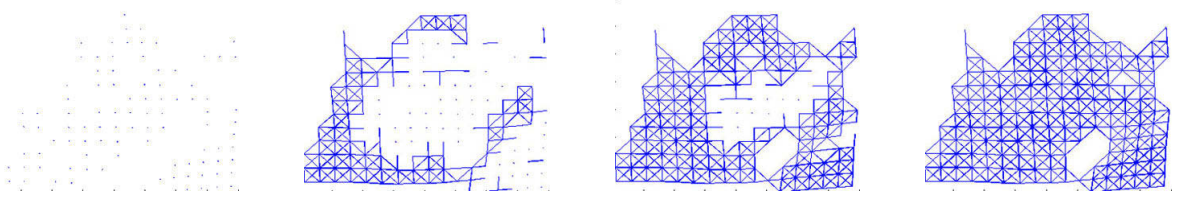

a) $r = 1$ (b) $r = 3$ (c) $r = 5$ (d) $r = 7$

Fig. 4. The *r*-SIG method applied to stereo vision sensor data for various values of *r*.

An extension of the SIG method is the automatic calculation of the bandwidth h from Eqns. (3) and (5). The local value of the bandwidth is critical to local surface smoothness. A small h value means that relatively few points influence

the surface at any one point, and the surface is therefore rough, as it would oscillate in an attempt to pass as nearly as possible through each point. Noise in the original data has a large impact on the resulting surface when a small bandwidth is used. An overly large bandwidth value results in the calculated surface being overly smooth relative to the actual part surface, and missing features all together. Klein's automatic bandwidth calculation adapts the value depending on the local point density of the data. However, we found that Klein's method actually decreases the smoothness of the resulting surface because the bandwidth value changes from point to point rather than progressing smoothly. Our new automatic bandwidth adjustment is done with a method based on Shepard's Interpolant [20], in which h is calculated as a continuous function of P_*, the estimated point on the surface, as seen in Eqn. (9). In this case d_i represents the distance to the r^{th} nearest neighbour of the point P_i, as it does with the r-SIG method.

$$h(P_*) = \frac{\sum_{i=1}^{N} d_i w_i^{-2}}{\sum_{i=1}^{N} w_i^{-2}} \tag{9}$$

The SIG method is feature size independent and works well for data sets with roughly uniform density, but its effectiveness depends heavily on the variation of the density of the data. Our automatic bandwidth calculation improves the SIG and r-SIG methods, but with the data sets gathered from actual parts the SIG fails. The importance of the parameter r in the r^{th} order SIG is shown in Fig. 4. Large holes are seen in the data in the case where $r = 3$; some of these holes are filled when $r = 5$ and the connectivity plot is much improved when $r = 7$. The increase in r is necessary due to the overlapping data gathered from the stereo vision sensor, as shown in Fig. 3. Eqn. (8), the SIG equation, is the criteria for when edge connections between points are made. If for example there are five points essentially overlapping, then the 5th nearest neighbour distance is very small. Therefore connections are only made between points which are very close together; the connections are between the same physical point on the part, which has been repeated and slightly offset due to the noise in each camera image. The automatic bandwidth calculation is based on the largest connecting edge within a local region, so detects only the short connections between very close points, which are too small a distance to be significant. Increasing the parameter r beyond the number of overlapping points causes the nearest neighbour distance to increase dramatically, to roughly the 2.54 mm grid distance between points on the undeformed sheet steel, and hence significantly improves the connectivity plot, as can be seen for the case when $r = 7$. The disadvantage of the r-SIG method with this type of real point cloud data is that the variation in local density of the points is unpredictable, and manual tests must be performed to determine the appropriate parameter. Also, although $r = 7$ might be required for one section of the data, another local area might need only a smaller r, in which case many additional, overly long and undesired connections are made between data points. The results of our WLS method using r-SIG with our improved automatic bandwidth adjustment are shown in Fig. 5. This is a 2D curve fitting example to simplify the display of results, with the data points and the resulting curve shown. In this case, $r = 2$ and Fig. 5(a) has two coincident data points at each location while Fig. 5(b) has these two data points slightly separated by introduced noise. Where data is duplicated and with $r = 2$, the surface is essentially a standard WLS with SIG fit, and the area of higher point density at the top of the point cloud set sees the curve miss the top feature entirely, but the straighter sections of the curve fit very well. When noise is introduced, the points are no longer duplicated and the surface better follows the top curve of the data, but is subject to more unevenness elsewhere. These results show the disadvantage of the SIG method in that it is very difficult to properly fit a surface to a data set of varying density with one value of r.

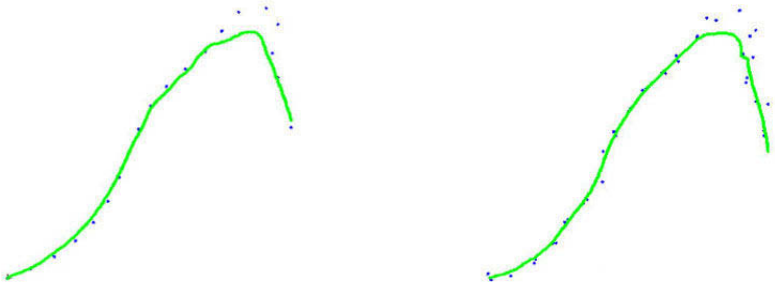

a) Duplicate data point with no noise (b) Introduced noise to separate data points

Fig. 5. The WLS r-SIG method with automatic bandwidth adjustment applied to a 2D data set with $r = 2$.

4. GAUSSIAN IMPLICIT SURFACE MODEL

We developed a further surface model due to the shortcomings of the proximity graph WLS implicit surface model when dealing with point cloud data of varying density. The Gaussian weighted least squares method is an extension of the standard WLS method with an improved distance kernel, replacing that of either Eqn. (3) or (5). The new Gaussian kernel, Eqn. (10), is a modification of that in Eqn. (3) that, rather than calculating the distance between a data point and the corresponding guess of the point on the surface, calculates d_i, the distance between two data points P_i and P_j, Eqn. (11). The parameter h is, as before, a feature parameter representing the nominal distance between grid points.

$$w_i = e^{-d_i^2/h^2} \tag{10}$$

$$d_i = \left\| P_i - P_j \right\| \tag{11}$$

We used the Gaussian method to model the surface of the same section of data as was used for the *r*-SIG method in Fig. 4. The nominal, undeformed grid separation distance for both the circular and the square grids is 2.54 mm, so results for three different bandwidth choices were plotted, as seen in Fig. 6: h = 2; h = 2.54; and h = 3. When h = 2, some data points in the areas of higher strain are close enough to other points to form some connections, but there are many gaps. When the nominal value of h = 2.54 is chosen the results are excellent, with nearly all points fully connected to other points and few overly long connections. Continuing work is being done to eliminate the long connections through stochastic pruning. Increasing the bandwidth to h = 3 significantly increases the number of connections made, beyond what is desirable.

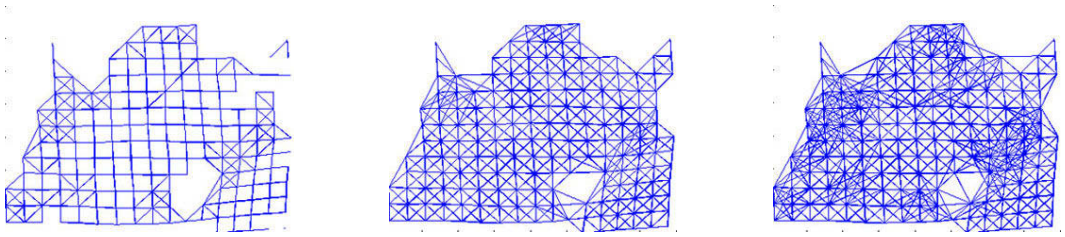

a) h = 2 (b) h = 2.54 (c) h = 3

Fig. 6. The Gaussian method applied to stereo vision sensor data for various values of h.

The examples show that with the Gaussian method proper selection of h is very important. Automatic bandwidth adjustment for the Gaussian WLS is similar to that for the *r*-SIG WLS presented in Eqn. (9). An initial guess for the bandwidth parameter is used to calculate the weights of each point in Eqn. (10), and then for each point P_i the new bandwidth parameter is calculated as the weighted sum of the distances to local points P_j, Eqn. (12). This new set of h_i values is used to calculate a generalized bandwidth function using the Shepard Interpolant, Eqn. (13), that is a measure of local density at any point in the space of the data set. For this calculation, an improved estimate of the weights is used, Eqn. (14).

$$h_i = \frac{\sum_{j=1}^{N} w_j d_j}{\sum_{j=1}^{N} w_j}, \; i \neq j \tag{12}$$

$$h(P_*) = \frac{\sum_{i=1}^{N} h_i w_i^{-2}}{\sum_{i=1}^{N} w_i^{-2}} \tag{13}$$

$$w_i = e^{-d_i^2/h_i^2}, \text{ where } d_i = \left\| P_* - P_i \right\| \tag{14}$$

The results of this Gaussian WLS with automatic bandwidth adjustment are very good with the point cloud data sets used. The Gaussian method does not depend on the density of the data, but does depend on the feature size of the local region of the part. Fig. 7 shows the results of our Gaussian WLS method with automatic bandwidth adjustment

applied to the same 2D data as was used with the *r*-SIG method in Fig. 5. Although a simplification, this data set produces results which are a good representation of the more complex data sets used in this paper, and as such is able to show the effectiveness of the Gaussian WLS method. For both the duplicate point and the noisy data sets, the Gaussian surface interpolation is able to follow the data very well for the length of the curve while remaining smooth. Some Gaussian shrinkage is evident at the peak; this problem is currently being examined.

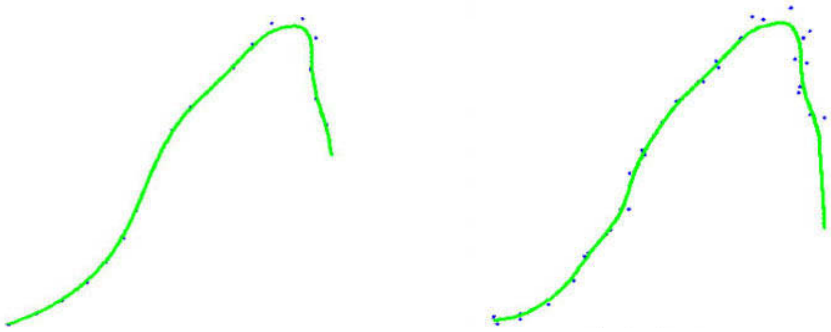

a) Duplicate data point with no noise (b) Introduced noise to separate data points

Fig. 7. The Gaussian WLS method with automatic bandwidth adjustment applied to a 2D data set.

5. INCORPORATING A SCALAR ATTRIBUTE

The speed of a process is becoming very important in modern manufacturing. As such, it is highly desirable to be able to quickly analyze some criteria of a part in addition to its geometry. One such criterion is the local strain of a stamped part, where it is convenient and efficient to be able to plot the thickness strain of the part directly onto its surface. For each point cloud data set used in this paper there is a scalar attribute, the thickness strain, in addition to the Cartesian coordinates at each point. This attribute adds a fourth dimension to the data, and our method plots the scalar on the implicit surface in a two step process. In the first step, a set of weights of the colours is developed, again using the Shepard Interpolant, as shown in Eqn. (15) and Eqn. (16). The scalar, in this case strain which will be represented by colour, is given the variable c_i. The equation for the distance d_i is a piecewise combination of an exponentially decreasing, infinitely supported curve with a second curve that converges to zero to ensure that the strain calculation is locally supported. The variable R represents the distance to convergence at zero of the curve.

$$w_i = \frac{\sum_{i=1}^{N} c_i d_i^{-2}}{\sum_{i=1}^{N} d_i^{-2}} \tag{15}$$

$$d_i = \begin{cases} 0\ , & r > R \\ \frac{81}{4R^4} r^2 - \frac{81}{2R^3} r + \frac{81}{4R^2}\ , & \frac{1}{3}R < r \le R \\ r^{-2}, & \text{otherwise} \end{cases} \tag{16}$$

Once the colour weights are calculated, they are used to compute a normal to a hyperplane $f(P_*)$ at each point on the surface using the WLS method, then we calculate a weighted linear combination of the hyperplanes as shown in Eqn. (17), which represents the colour as a function of P_*.

$$C(P_*) = \sum w_i f(P_*) \tag{17}$$

To display the results of the colour algorithm, a 2D data set with the scalar attribute as one of the dimensions was created, and the implicit surface model and colour models were developed. Fig. 8 shows this result, with the oscillating line representing Shepard's Interpolant, which is used as the weighting function, and the smoother line showing the resultant smoothed scalar attribute interpolant.

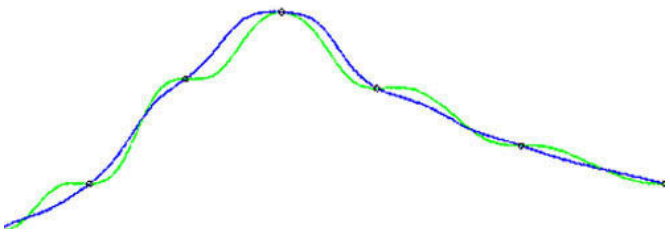

Fig. 8. 2D data set with colour attribute as one dimension.

6. RESULTS

The methods discussed serve to improve the ability of implicit surface models to properly fit the surface which represents an unorganized, noisy point cloud of data and to fit a scalar attribute to the resulting surface. In this case, measurements of the local thickness strain are used to produce 3D, colour temperature plot style representations of the strain over the surface of a stamped sheet metal part. The results are shown in Fig. 9, which includes both a detailed view of one corner of the stereo vision data set and a full view of the laser digitizer data set shown in Fig. 2. The methods described are useful for visualization purposes, but it is clear from the image on the left side of Fig. 9 that the scalar mapping is not smooth. We are currently working on smoothing both the surface reconstruction and the scalar mapping, which is an area of little existing work.

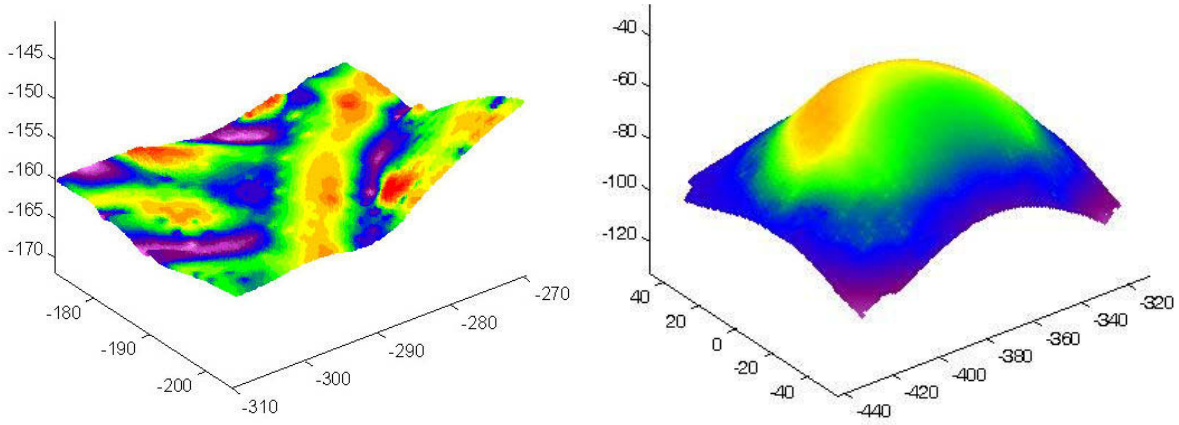

Fig. 9. Results of 3D WLS with colour strain scalar attribute.

7. CONCLUSIONS

We have presented both improvements to existing proximity graph based implicit surface definitions and a new Gaussian surface definition. New developments were required to improve the results when using noisy point cloud data acquired from the scanning of actual parts. The laser digitizer and the stereo vision data acquisition systems each present their own specific difficulties with the data sets that lead to the failure of previous surface fit methods. The improved SIG based method is better at dealing with these problems and includes a smoother automatic bandwidth calculation, but the SIG method is not well suited to data with widely varying density of the type that is found with the point clouds used. A new Gaussian method is much better suited to data with these variations in density and also includes automatically adjusting bandwidth. The addition of a scalar to 3D point cloud data effectively creates a four-dimensional problem. The scalar used in this case is thickness strain data gathered in conjunction with the Cartesian coordinates by the 3D scanning systems, but other scalars such as grey scale intensity, used to represent the colours of the part, could be used. The scalar is used to fit a temperature plot type of colour interpretation of the strain data over the implicitly defined surface to allow for fast and easy recognition of the strain of a stamped part. Continuing work includes the smoothing of both the surface fit and the colour algorithms and the implementation of the surface reconstruction into a complete laser scanner based dimensional inspection system.

8. ACKNOWLEDGEMENTS

Equipment funding and graduate student stipends for this work were provided by the Natural Sciences and Engineering Research Council of Canada (NSERC). Philip Mitchell and Harley Chan provided the stereo vision and laser digitizer data respectively. Allan Spence was a great help with concepts and ideas. In addition, we would like to thank the CAD'06 initial reviewer for their detailed review and helpful comments.

9. REFERENCES

[1] Ahn, S. J., Rauh, W., Cho, H. S. and Warnecke, H.-J., Orthogonal Distance Fitting of Implicit Curves and Surfaces, *IEEE Transactions on Pattern Analysis and Machine Intelligence*, Vol. 24, No. 5, 2002, pp 620-638.

[2] Ahn, S. J., *Least Squares Orthogonal Distance Fitting of Curves and Surfaces in Space*, Springer, Berlin Heidelberg, 2005.

[3] Bajaj, C. L., Bernardini, F. and Xu, G., Reconstructing Surfaces and Functions on Surfaces from Unorganized Three-Dimensional Data, *Algorithmica*, Vol. 19, Nos. 1-2, 1997, pp 243-261.

[4] Boyer, E., Lister, L. and Shader, B., Sphere-of-Influence Graphs Using the Sup-Norm, *Mathematical and Computer Modelling*, Vol. 32, No. 10, 2000, pp 1071-1082.

[5] Carr, J. C., Fright, W. R. and Beatson, R. K., Surface Interpolation with Radial Basis Functions for Medical Imaging, *IEEE Transactions on Medical Imaging*, Vol. 16, No. 1, 1997, pp 96-107.

[6] Carr, J. C., Beatson, R. K., Cherrie, J. B., Mitchell, T. J., Fright, W. R., McCallum, B. C. and Evans, T. R., Reconstruction and Representation of 3D Objects with Radial Basis Functions, *Proceedings of the SIGGRAPH '01*, 2001, pp 67-76.

[7] Chan, H. L., Mitchell, J. P., Spence, A. D., Sklad, M. P. and Capson, D. W., Laser Digitizer / Stereo Vision Methods for Simultaneous Measurement / Analysis of Sheet Metal Forming Strain / Geometry, *Proceedings of IMECE05 – IMECE2005-79216*, 2005.

[8] Gauss, C. F., *Theory of Motion of the Heavenly Bodies Moving About the Sun in Conic Sections*, first published 1809, translation by C. F. Davis, Dover, New York, N.Y., 1963.

[9] Hoppe, H., DeRose, T., Duchamp, T., McDonald, D. and Stuetzle, W., Surface Reconstruction from Unorganized Points, *Computer Graphics*, Vol. 26, No. 2, 1992, pp 71-78.

[10] Jaromczyk, J. W. and Toussaint, G. T., Relative Neighborhood Graphs and Their Relatives, *Proceedings of the IEEE*, Vol. 80, No. 9, 1992, pp 1502-1517.

[11] Klein, J. and Zachmann, G., Point cloud surfaces using geometric proximity graphs, *Computers & Graphics*, Vol. 28 No. 6, 2004, pp 839-850.

[12] Lee, I.-K., Curve reconstruction from unorganized points, *Computer Aided Geometric Design*, Vol. 17 No. 2, 2000, pp 161-177.

[13] Levin, D., The Approximation Power of Moving Least Squares, *Mathematics of Computation*, Vol. 67, No. 224, 1998, pp 1517-1531.

[14] Levin, D., Mesh-Independent Surface Interpolation, *Geometric Modeling for Scientific Visualization*, Springer-Verlag, Berlin Heidelberg, 2004, pp 37-49.

[15] McLain, D. H., Drawing contours from arbitrary data points, *The Computer Journal*, Vol. 17, 1974, pp 318-324.

[16] McLain, D. H., Two dimensional interpolation from random data, *The Computer Journal*, Vol. 19, 1976, pp 178-181.

[17] Michael, T. S. and Quint, T., Sphere of influence graphs and the L_∞-metric, *Discrete Applied Mathematics*, Vol. 127, No. 3, 2003, pp 447-460.

[18] Pfister, H., Zwicker, M., van Baar, J. and Gross, M., Surfels: Surface Elements as Rendering Primitives, *Proceedings of the SIGGRAPH '00*, 2000, pp 335-342.

[19] Rusinkiewicz, S. and Levoy, M., QSplat: A Multiresolutional Point Rendering System for Large Meshes, *Proceedings of the SIGGRAPH '00*, 2000, pp 343-352.

[20] Shepard, D., A two-dimensional interpolation function for irregularly-spaced data, *Proceedings of the ACM 1968*, 1968, pp 517-524.

[21] Spence, A. D., Chan, H.-L., Mitchell, J. P. and Capson, D. W., Automotive Sheet Metal and Grid Digitizing Solutions, *Computer Aided Design & Applications*, Vol. 2, Nos. 1-4, 2005, pp 135-144.